

Stability analysis of twist grain boundaries in lamellar phases of block copolymers

Xusheng Zhang¹, Zhi-Feng Huang^{1,2}, Jorge Viñals¹

¹*McGill Institute for Advanced Materials, and Department of Physics,
McGill University, Montreal, QC H3A 2T8, Canada*

²*Department of Physics and Astronomy,
Wayne State University, Detroit, MI 48201*

(Dated: November 5, 2018)

Abstract

Twist grain boundaries are widely observed in lamellar phases of block copolymers. A mesoscopic model of the copolymer is used to obtain stationary configurations that include a twist grain boundary, and to analyze their stability against long wavelength perturbations. The analysis presented is valid in the weak segregation regime, and includes direct numerical solution of the governing equations as well as a multiple scale analysis. We find that a twist boundary configuration with arbitrary misorientation angle can be well described by two modes, and obtain the equations for their slowly varying amplitudes. The width of the boundary region is seen to scale as $\epsilon^{-1/4}$, with ϵ being the dimensionless distance to the order-disorder transition. We finally present the results of the linear stability analysis of the planar boundary.

PACS numbers: 47.54.-r.61.25.H-.83.50.-v.05.45.-a

I. INTRODUCTION

Block copolymers are being explored for either direct use or as processing templates in nanolithography, photonic devices, high density storage systems, or drug delivery, just to name a few examples [1, 2, 3, 4]. Self assembly into mesophases of different symmetries and of controllable periodicity (typically at the nanoscale) makes these materials a very versatile tool, and hence the interest in studying their architectures and self assembly mechanisms [1, 2]. A common practical limitation to widespread use, however, is the considerable difficulty encountered in producing well ordered microstructures [3, 5, 6, 7]. Given that the longest relaxation times of partially ordered microstructures are often controlled by existing topological defects, much attention has been paid to the motion of disclinations [5, 8] and grain boundaries in lamellar [9, 10] and cylindrical phases [11].

Theoretical analyses of defect motion have been based on a mesoscopic description of a copolymer melt which is valid for characteristic time scales much longer than the slowest relaxation time of the polymer chain [12, 13, 14]. Asymptotic methods commonly employed in studies of defect dynamics in systems outside of equilibrium [15] have been applied, to tilt grain boundaries in lamellar phases [16, 17]. This type of boundary separates two domains of differently oriented lamellae such that the plane formed by lamellar normals of the two domains is perpendicular to the boundary plane. Examples include boundary migration induced by lamellar curvature [9, 18, 19] and the effect of an imposed shear flow [20, 21].

In three-dimensional samples, 90° tilt boundary configurations (the so called T-junctions) are rarely observed in experiments [22], possibly because they are generically unstable [23]. On the other hand, twist boundaries (such that the wavevectors of both adjacent lamellar domains lie on the boundary plane (see Fig. 1)) of various misorientation angles are commonly observed [24, 25, 26]. Nevertheless, analyses of their structure and stability are still very limited [27, 28, 29].

We focus in this paper on a coarse grained model of a twist grain boundary, leading to the associated amplitude (or envelope) equation description. We obtain a stationary profile comprising a twist grain boundary, and numerically compute its linear stability. Our results are based on the Leibler or Swift-Hohenberg model [12, 30], valid in the limit of weak segregation. The analysis is conducted for a boundary of arbitrary misorientation angle α . In contrast with the results obtained for the case of tilt grain boundaries, we find that the

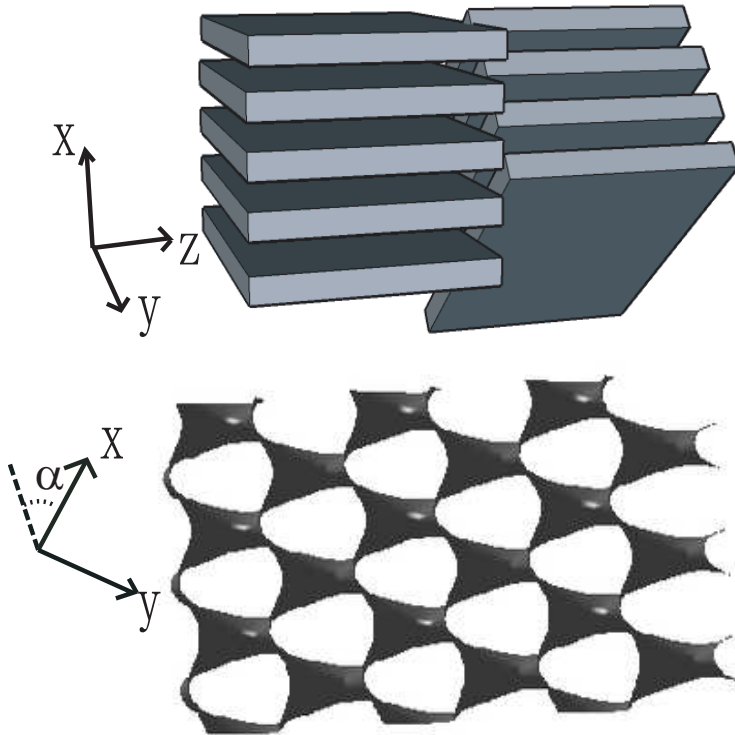


FIG. 1: Schematic of a twist grain boundary separating two lamellar domains with a misorientation angle α . Also shown (bottom) is the morphology at the boundary as given by the order parameter of the model.

twist boundary width scales as $\epsilon^{-1/4}$, with ϵ the dimensionless distance to the order-disorder threshold, and that the twist boundary is linearly stable to long wavelength modulations for any angle α , consistent with experimental findings in copolymer melts.

II. MODEL

A. Coarse-grained model equation

At a mesoscopic level, a weakly segregated diblock copolymer melt close to the order-disorder transition temperature T_{ODT} is described by a free energy, function of monomer composition, given by Leibler [12, 31]. The corresponding relaxational dynamics leads to the Swift-Hohenberg model equation [14, 15, 30]. For a symmetric diblock melt (with equal volume fraction of the two constituent monomers), this model equation is (in dimensionless

units)

$$\frac{\partial \psi}{\partial t} = \epsilon \psi - (\nabla^2 + q_0^2) \psi - \psi^3, \quad (1)$$

where the order parameter field ψ represents the local density difference between the two monomers of the diblock, and $q_0 = 1$ after rescaling, although we retain the symbol q_0 in what follows for clarity of presentation. As already stated above, the control parameter ϵ measures the distance from the order-disorder transition or bifurcation point at which $\epsilon = 0$. For $\epsilon > 0$ (temperature below T_{ODT}), a pattern with lamellar symmetry emerges, although usually accompanied with large amount of defects. Therefore typical configurations display a multidomain microstructure.

B. Amplitude equations of twist grain boundaries

Following the standard multiple scale approach in the weak segregation limit [15, 17], we can separate the fast spatial/temporal scales of a base lamellar pattern from its slowly varying amplitude, and derive the associated amplitude equations for a twist grain boundary. The derivation is based on the method given in Ref. [21]. The order parameter field ψ is expanded as the superposition of two base modes

$$\psi = \frac{1}{\sqrt{3}} [A \exp(i\vec{q}_1 \cdot \vec{r}) + B \exp(i\vec{q}_2 \cdot \vec{r}) + \text{c.c.}], \quad (2)$$

where $\vec{q}_1 = q_0 \hat{x}$ and $\vec{q}_2 = q_0 (\cos \alpha \hat{x} + \sin \alpha \hat{y})$ (with α the twist angle) are the orientations of two domains adjacent the twist boundary (see Fig. 1). The evolution of the complex amplitudes A and B is governed by (to leading order in $\mathcal{O}(\epsilon^{3/2})$)

$$\partial_t A = \left[\epsilon - (\nabla_{\parallel 1}^2 + 2iq_0 \partial_{\vec{n}_1})^2 \right] A - |A|^2 A - 2|B|^2 A, \quad (3)$$

$$\partial_t B = \left[\epsilon - (\nabla_{\parallel 2}^2 + 2iq_0 \partial_{\vec{n}_2})^2 \right] B - |B|^2 B - 2|A|^2 B, \quad (4)$$

where \vec{n}_1, \vec{n}_2 are the normals to the lamellar planes in domains A and B respectively, $\nabla_{\parallel 1}^2$ is the the Laplacian operator on the lamellar plane of domain A, and $\nabla_{\parallel 2}^2$ represents the Laplacian operator on the lamellar plane of domain B. For instance, if $\vec{n}_1 = \hat{x}$ (i.e. $\vec{q}_1 = q_0 \hat{x}$), $\nabla_{\parallel 1}^2 = \partial_y^2 + \partial_z^2$ and $\partial_{\vec{n}_1} = \partial_x$.

III. STATIONARY TWIST GRAIN BOUNDARY CONFIGURATION

The steady state configuration of twist grain boundaries has been first examined through direct numerical solution of the model equation (1). A pseudospectral method in Fourier space is adopted, with periodic boundary conditions in all three directions. A Crank-Nicholson time stepping scheme is applied to the linear terms, with a second order Adams-Bashford algorithm used for the nonlinear term. Periodic boundary conditions are satisfied through the consideration of an initial configuration comprising a symmetric pair of twist boundaries that are sufficiently far apart so that their motion is approximately independent. An additional restriction needs to be placed on the dimension of the computational cell along the x and y directions on the plane of the grain boundary (as shown schematically in Fig. 2). Due to the requirement that an integer multiple of lamellar periods λ_0 ($= 2\pi/q_0$) must equal the length of the computational cell in the direction parallel to the lamellar normal, the unit cell lengths are $l_x = \lambda_0/\sin(\alpha/2)$ and $l_y = \lambda_0/\cos(\alpha/2)$. We consider a uniform spatial discretization in a $L_x \times L_y \times L_z$ grid with spacings $\Delta x = l_x/16$, $\Delta y = l_y/16$, and $\Delta z = \lambda_0/16$, corresponding to 16 grid points per unit cell length. Most calculations shown below correspond to a system size of 256^3 , with a dimensionless time step $\Delta t = 0.2$ used in the numerical integration.

A typical stationary configuration is shown in Fig. 3, corresponding to $\alpha = 90^\circ$ with $\epsilon = 0.04$ and at a time $t = 10^4$. Also shown in the figure (in grey scale) is the two dimensional order parameter at the boundary interface. It is doubly periodic along the two directions defined by the bulk lamellar domains adjacent to the grain boundary.

Before we carry out a multiple scale analysis, we have checked the underlying assumption that the stationary order parameter field ψ can be decomposed into two Fourier modes (see Eq. (2)). We calculate the Fourier spectrum of the order parameter field both at the grain boundary and in the bulk. We illustrate our findings with the case of a $\alpha = 75^\circ$ twist boundary with $\epsilon = 0.02$. The two dimensional Fourier spectrum of ψ on the boundary plane ($z = (59/256)L_z$) shows four maxima at wavevectors $(\pm q_{x0}, \pm q_{y0})$, with $\sqrt{q_{x0}^2 + q_{y0}^2} = q_0$ (q_0 is the wavenumber in the bulk). We also observe $2 \arctan(q_{x0}/q_{y0}) = 75^\circ$ (exactly the misorientation angle α). This reflects the fact that the order parameter in the grain boundary region is a combination of the two bulk modes. The same conclusion is supported by an analysis of higher harmonics in the spectrum. Figures 4a and 4b show the intensity of the

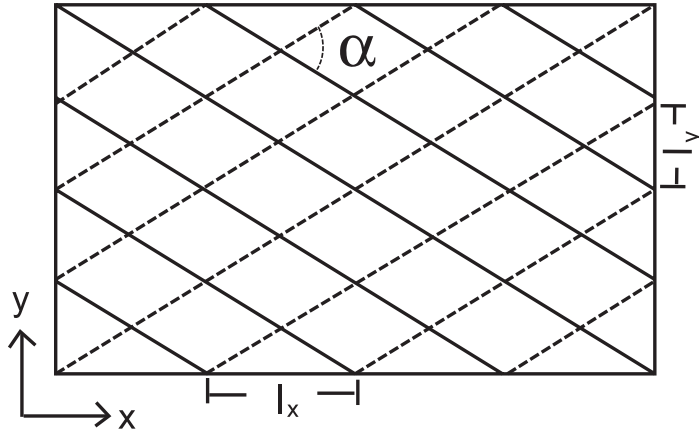


FIG. 2: Schematic of the constraint imposed by periodic boundary conditions. Solid and dashed lines represent two misoriented lamellar layers at the grain boundary. In order to accommodate two domains with a relative misorientation α and use periodic boundary conditions, one needs to choose as unit cells dimensions $l_x = \lambda_0 / \sin(\alpha/2)$, $l_y = \lambda_0 / \cos(\alpha/2)$ along the x and y directions on the boundary plane.

spectrum along q_x at $q_y = q_{y0}$ and at two different values of z : one within the grain boundary (Fig. 4a), the other in the bulk A phase (Fig. 4b) (identical conclusions can be drawn from the analysis in phase B). Figures 4c and 4d show the same quantity but as a function of q_y at $q_x = q_{x0}$, and for the same two values of z . The fact that all the visible harmonics within the grain boundary region are almost the same as in the bulk suggests that in the weak segregation limit considered here, the superposition of the two bulk modes in Eq. (2) used for the multiple scale analysis that will follow appears to be sufficient for the description of the order parameter profile around the grain boundary.

IV. ASYMPTOTIC BOUNDARY WIDTH

The boundary width δ of a twist grain boundary as a function of ϵ in the limit $\epsilon \rightarrow 0$ can be determined either numerically from the stationary configuration given above, or via a multiple scale analysis (3) and (4). In the latter case, simple dimensional analysis of Eqs.

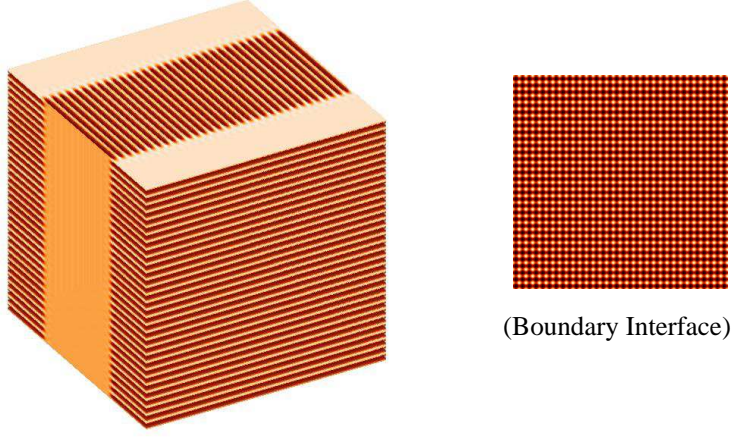


FIG. 3: A stationary $\alpha = 90^\circ$ twist grain boundary configuration in a lamellar phase, as given by numerical solution of the model equation (1). The grid size is 256^3 , and $\epsilon = 0.04$. Right panel: order parameter (gray scale) at the boundary interface.

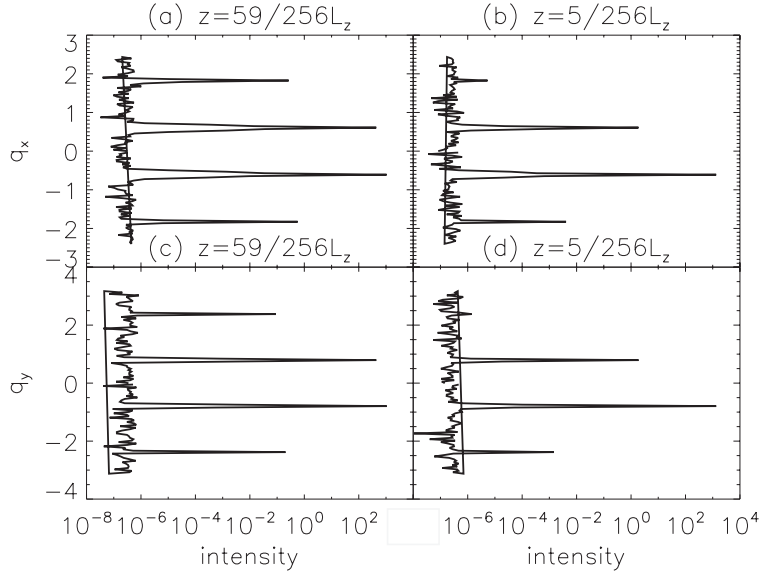


FIG. 4: Power spectrum of ψ along specific directions in $\vec{q} = (q_x, q_y)$ space, and at constant location z for a $\alpha = 75^\circ$ twist boundary. We show the spectrum for $\epsilon = 0.02$ and $t = 2000$. Panel (a) shows the power spectrum as a function of q_x for $q_y = q_{y0}$ and $z = (59/256)L_z$, whereas (b) shows the spectrum far into the bulk at $z = (5/256)L_z$. Panels (c) and (d) show similar spectra as a function of q_y for $q_x = q_{x0}$ and at $z = (59/256)L_z$ (c) or $(5/256)L_z$ (d). Here (q_{x0}, q_{y0}) is the location of the peak of the two dimensional power spectrum for the order parameter ψ .

(3) and (4) along the grain boundary normal (the z direction) leads to the following result

$$\delta \sim \epsilon^{-1/4}. \quad (5)$$

This is in contrast with the known behavior for a tilt grain boundary in which $\delta \sim \epsilon^{-1/2}$ [16]. The latter scaling behavior follows from the fact that there are two distinct characteristic length scales for lamellar relaxation: One along the direction parallel to the lamellar normal with scale $l_{\perp} \propto \epsilon^{-1/2}$, the other along the plane of the lamella with scale $l_{\parallel} \propto \epsilon^{-1/4}$. For a twist grain boundary, on the other hand, the direction (z) normal to the boundary is parallel to the lamellar planes of both phases, and hence it is reasonable to expect that the boundary width along z scales as $\epsilon^{-1/4}$. In summary, a twist boundary is much narrower than a tilt boundary in the limit $\epsilon \rightarrow 0$.

The result above holds for any misorientation angle as we have verified by numerical solution of the model equation (1). We first determine the location of the boundary by estimating the amplitude $B(z)$ [21]

$$B(z) \simeq \frac{\sqrt{3}}{4N} \sum_{m=1}^N [\psi(\vec{r} \cdot \hat{n}_B = m\lambda_0; z) - \psi(\vec{r} \cdot \hat{n}_B = (m - 1/2)\lambda_0; z)], \quad (6)$$

with \hat{n}_B the unit normal to lamellae B and N the number of pairs of lamellae. The boundary region is chosen such that the value of $B(z)$ lies within 10% – 90% of its maximum. Since the width of the boundary is only several times the lamellar width, a linear interpolation algorithm is used to increase the accuracy of the boundary location. The relation obtained between boundary width δ (in dimensionless units) and misorientation angle α is plotted in Fig. 5 for $\epsilon = 0.02$. For $\alpha > 20^\circ$, the boundary width becomes approximately independent of α . Otherwise, δ increases rapidly with decreasing angle. Although the accuracy of our numerical solution degrades when α is small, the trend obtained points to a divergence of the boundary width as $\alpha \rightarrow 0$. We find similar results when numerically solving the corresponding amplitude equations (3) and (4) for small twist angles. Figure 5 also shows our results for δ as a function of ϵ for $\alpha = 90^\circ$. Given the spatial discretization used in our integration, the boundary widths that we have been able to investigate range from $3\lambda_0$ at $\epsilon = 0.001$ to $3\lambda_0/4$ at $\epsilon = 0.4$ (with $\lambda_0 = 2\pi/q_0$). Within this limited range, a power law dependence between δ and ϵ is found, with an exponent -0.244 ± 0.002 , in agreement with our expectation from dimensional analysis. Analogous results have been obtained for other values of α .

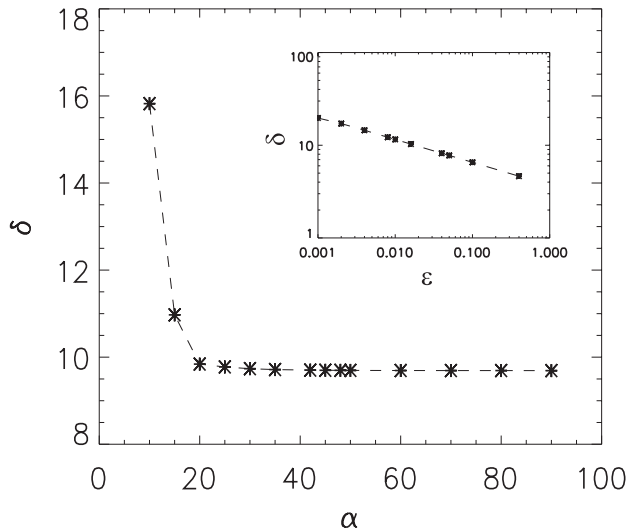


FIG. 5: Boundary width δ (in dimensionless units) as a function of twist angle α for $\epsilon = 0.02$. Inset: Width δ vs. ϵ as obtained from the stationary solutions of Eq. (1) for $\alpha = 90^\circ$. The slope of the log-log plot is -0.244 ± 0.002 .

V. STABILITY ANALYSIS

As noted above, twist grain boundaries are observed in great abundance in experiments that address the microstructure of large samples in the lamellar phase [24, 25, 26]. We conduct here a linear stability analysis of a planar boundary from the amplitude equations (3) and (4) that are derived from our model equation. We start from a base state involving a stationary and planar twist boundary of arbitrary misorientation angle α and wavenumber q_0 [32]. The corresponding amplitudes $A^{(0)}$ and $B^{(0)}$ are assumed to be only a function of z , the direction normal to the boundary, and are given by

$$\epsilon A^{(0)} - \partial_z^4 A^{(0)} - |A^{(0)}|^2 A^{(0)} - 2|B^{(0)}|^2 A^{(0)} = 0, \quad (7)$$

$$\epsilon B^{(0)} - \partial_z^4 B^{(0)} - |B^{(0)}|^2 B^{(0)} - 2|A^{(0)}|^2 B^{(0)} = 0. \quad (8)$$

We next expand the complex amplitudes around the stationary solutions

$$A(x, y, z, t) = A^{(0)}(z) + \sum_{q_x, q_y} \hat{A}(q_x, q_y, z, t) e^{i(q_x x + q_y y)}, \quad (9)$$

$$B(x, y, z, t) = B^{(0)}(z) + \sum_{q_x, q_y} \hat{B}(q_x, q_y, z, t) e^{i(q_x x + q_y y)}, \quad (10)$$

substitute these expansions into Eqs. (3) and (4), and linearize the resulting equations with respect to the perturbations \hat{A} and \hat{B} . We find

$$\begin{aligned} \partial_t \hat{A}(q_x, q_y, z, t) &= [\epsilon - (\partial_z^2 - q_y^2 - 2q_0 q_x)^2 - 2|A^{(0)}|^2 - 2|B^{(0)}|^2] \hat{A}(q_x, q_y, z, t) \\ &\quad - (A^{(0)})^2 \hat{A}^*(-q_x, -q_y, z, t) - 2A^{(0)} B^{(0)*} \hat{B}(q_x, q_y, z, t) \\ &\quad - 2A^{(0)} B^{(0)} \hat{B}^*(-q_x, -q_y, z, t), \end{aligned} \quad (11)$$

$$\begin{aligned} \partial_t \hat{B}(q_x, q_y, z, t) &= [\epsilon - (\partial_z^2 - q_{y2}^2 - 2q_0 q_{x2})^2 - 2|A^{(0)}|^2 - 2|B^{(0)}|^2] \hat{B}(q_x, q_y, z, t) \\ &\quad - (B^{(0)})^2 \hat{B}^*(-q_x, -q_y, z, t) - 2B^{(0)} A^{(0)*} \hat{A}(q_x, q_y, z, t) \\ &\quad - 2A^{(0)} B^{(0)} \hat{A}^*(-q_x, -q_y, z, t), \end{aligned} \quad (12)$$

where $q_{x2} = \cos \alpha q_x + \sin \alpha q_y$ and $q_{y2} = -\sin \alpha q_x + \cos \alpha q_y$.

Since we do not have an analytic expression for the amplitudes of the base state, we study its stability by examining the temporal evolution of small random perturbations to both real and imaginary parts of \hat{A} and \hat{B} for a range of values of q_x and q_y , and integrating the system of Eqs. (7)–(12) numerically. The details of the numerical algorithm and procedure are given in Ref. [23]. The parameters chosen here are $\Delta z = \lambda_0/8$ for the discretization along the z direction, with $L_z = 1024$ grid nodes (or equivalently a length of the computational domain of $128\lambda_0$). The time step chosen is $\Delta t = 0.2$. If the planar grain boundary is stable, perturbations in \hat{A} and \hat{B} will decay in time for all wavevectors (q_x, q_y) ; otherwise an instability would manifest itself by an increase of these perturbations within a certain range of wavevectors.

From the relaxation of the perturbations, we estimate the perturbation growth rate $\sigma(q_x, q_y)$ from $|\hat{A}(t)|, |\hat{B}(t)| \propto e^{\sigma(q_x, q_y)t}$ and the numerical solutions for \hat{A} and \hat{B} for a given set of (q_x, q_y) . A typical result is shown in Fig. 6 for $\alpha = 90^\circ$ and $\epsilon = 0.04$. We always observe that $\sigma < 0$, for all the wavevectors of the perturbation explored. This is also the case for different values of ϵ and angle α , as shown in Fig. 7. The maxima of σ for α ranging from 30° to 90° , and ϵ from 0.005 to 0.08 have been calculated, all yielding a stable planar boundary.

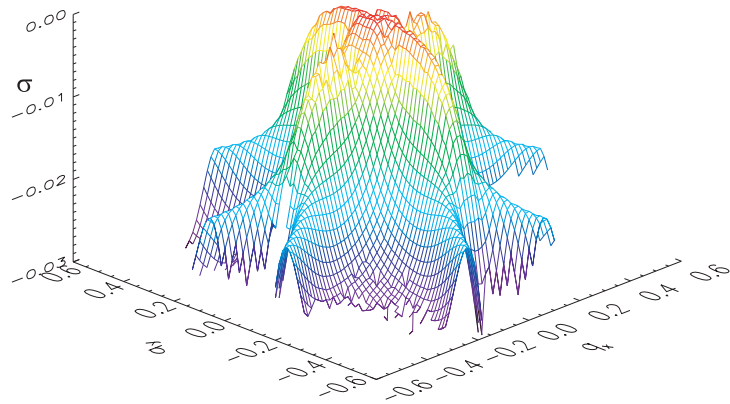


FIG. 6: Perturbation growth rate σ as a function of wavevector (q_x, q_y) for $\epsilon = 0.04$ and $\alpha = 90^\circ$.

We find that $\sigma < 0$ over the whole range of wavevectors investigated.

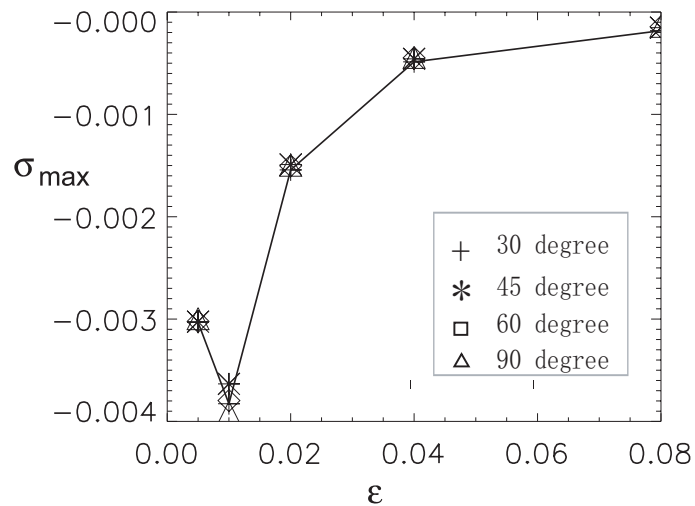


FIG. 7: Maximum perturbation growth rate σ_{\max} as a function of ϵ , for different twist angles $\alpha = 30^\circ, 45^\circ, 60^\circ$, and 90° .

VI. CONCLUSIONS

We have used the Swift Hohenberg model as an approximate mesoscale description for the evolution of a twist grain boundary in a lamellar phase of a diblock copolymer. We have shown that the order parameter field can be well approximated in the weak segregation

regime by a combination of the two modes of the ordered lamellar phases on either side of the grain boundary. The equations governing the slow evolution of the amplitudes or envelopes of these modes have been derived for arbitrary misorientation angle. The stationary solution is only a function of the coordinate normal to the grain boundary plane, and is characterized by a width $\delta \sim \epsilon^{-1/4}$, with ϵ the distance from the order-disorder point. We have then conducted a linear stability analysis by direct numerical solution of the governing equations, and have found that the twist boundary is linearly stable within a wide range of parameters investigated.

Acknowledgments

This research has been supported by the National Science Foundation under grant DMR-0100903, and by NSERC Canada.

-
- [1] S. B. Darling, *Prog. Polym. Sci.* **32**, 1152 (2007).
 - [2] C. Park, J. Yoon, and E. Thomas, *Polymer* **44**, 7779 (2003).
 - [3] C. Black, *Appl. Phys. Lett.* **87**, 163116 (2005).
 - [4] J. Yoon, W. Lee, and E. Thomas, *Nano Lett.* **6**, 2211 (2006).
 - [5] C. Harrison, D. Adamson, Z. Chen, J. Sebastian, S. Sethuraman, D. Huse, R. Register, and P. Chaikin, *Science* **290**, 1558 (2000).
 - [6] S. Kim, H. Solak, M. Stoykovich, N. Ferrier, J. de Pablo, and P. Nealy, *Nature* **424**, 411 (2003).
 - [7] E. Kramer, *Nature* **437**, 824 (2005).
 - [8] C. Harrison, D. Angelescu, M. Trawick, Z. Chen, D. Huse, P. Chaikin, D. Vega, J. Sebastian, R. Register, and D. Adamson, *Europhys. Lett.* **67**, 800 (2004).
 - [9] D. Boyer and J. Viñals, *Phys. Rev. E* **65**, 046119 (2002).
 - [10] Z.-F. Huang and J. Viñals, *J. Rheol.* **51**, 99 (2007).
 - [11] D. Boyer and J. Viñals, *Phys. Rev. Lett.* **89**, 055501 (2002).
 - [12] L. Leibler, *Macromolecules* **13**, 1602 (1980).
 - [13] T. Ohta and K. Kawasaki, *Macromolecules* **19**, 2621 (1986).

- [14] G. Fredrickson, *J. Rheol.* **38**, 1045 (1994).
- [15] M. Cross and P. Hohenberg, *Rev. Mod. Phys.* **65**, 851 (1993).
- [16] G. Tesauro and M. Cross, *Phil. Mag. A* **56**, 703 (1987).
- [17] P. Manneville, *Dissipative Structures and Weak Turbulence* (Academic, New York, 1990).
- [18] D. Boyer and J. Viñals, *Phys. Rev. E* **63**, 061704 (2001).
- [19] D. Boyer and J. Viñals, *Phys. Rev. E* **64**, 050101(R) (2001).
- [20] Z.-F. Huang, F. Drolet, and J. Viñals, *Macromolecules* **36**, 9622 (2003).
- [21] Z.-F. Huang and J. Viñals, *Phys. Rev. E* **69**, 041504 (2004).
- [22] S. Gido and E. Thomas, *Macromolecules* **27**, 6137 (1994).
- [23] Z.-F. Huang and J. Viñals, *Phys. Rev. E* **71**, 031501 (2005).
- [24] E. L. Thomas, D. M. Anderson, C. S. Henkee, and D. Hoffman, *Nature* **334**, 598 (1988).
- [25] S. P. Gido, J. Gunther, E. L. Thomas, and D. Hoffman, *Macromolecules* **26**, 4506 (1993).
- [26] S. P. Gido and E. L. Thomas, *Macromolecules* **27**, 849 (1994).
- [27] R. D. Kamien and T. C. Lubensky, *Phys. Rev. Lett.* **82**, 2892 (1999).
- [28] D. Duque and M. Schick, *J. Chem. Phys.* **113**, 5525 (2000).
- [29] A. V. Kyrylyuk and J. G. E. M. Fraaije, *Macromolecules* **38**, 8546 (2005).
- [30] J. Swift and P. Hohenberg, *Phys. Rev. A* **15**, 319 (1977).
- [31] G. H. Fredrickson and E. Helfand, *J. Chem. Phys.* **87**, 697 (1987).
- [32] The stability analysis presented in this paper concerns only base states of wavenumber q_0 . Twist grain boundaries separating uniform domains of wavenumber $q \neq q_0$ can be unstable. The range of stability as a function of q , at fixed ϵ , is smaller than that of uniform domains. Therefore there is a range of wavenumbers within which the instability originates in the grain boundary region.